



# Centrifuge Model Tests of Basal Reinforcement Effects on Geosynthetic-Reinforced Pile-Supported Embankment

Chao Xu<sup>1</sup>, Di Wu<sup>2(✉)</sup>, Shitong Song<sup>1</sup>, and Baochen Liu<sup>2</sup>

<sup>1</sup> Key Laboratory of Geotechnical and Underground Engineering of Ministry of Education, Tongji University, Shanghai 200092, China

<sup>2</sup> College of Architecture and Transportation Engineering, Guilin University of Electronic Technology, Guilin 541004, China  
wudi@guet.edu.cn

**Abstract.** As an effective and economical structure, geosynthetic-reinforced pile-supported (GRPS) embankment has been used in the construction of roadbed of railway and highway in soft soil area. Its key load transfer mechanism includes the soil arching effect of the embankment fill and the tensioned membrane effect of reinforcement in the mattress. Via these two effects, more embankment load is carried by piles, and the total settlement and differential settlement of the roadbed can be under control. Four centrifuge model tests were conducted to study the reinforcement effect of geosynthetic on embankment stability and pile efficacy. The following results are achieved: the surface settlement and differential settlement of embankment could be effectively reduced through appropriate setting of reinforced mattress; Basal reinforcement increased the pile efficacy and was affected by the number of reinforcement layers; The tensile force of geogrid below the embankment shoulder was larger than that near the road center because of the lateral restraint of basal reinforcement.

**Keywords:** Geosynthetic-reinforced and pile-supported (GRPS) embankment  
Geogrid · Basal reinforcement · Membrane effect · Arching effect  
Centrifuge model test

## 1 Introduction

As compared with some other ground improvement methods, geosynthetic-reinforced pile-supported (GRPS) embankments can be constructed quickly, do not require soft soil replacement and staged construction, and meet strict settlement requirements. Therefore, they become one of the favorable technologies for the construction of embankments on soft soil foundations. GRPS embankment, consisting of embankment fill, geosynthetic reinforcement, piles, and foundation soils, is a complex soil-structure system. The interaction among these components determines the load distribution and the functions exerted by the reinforcement. Its key load transfer mechanisms include soil arching and tensioned membrane effects and subsoil resistance.

Soil arching effect has been one of the intensive research topics in the study of GRPS embankment. Hewlett and Randolph [1] observed arching through a glass case

and proved that the arch was close to hemisphere form between square lay-out piles. Other model tests (Low et al. [2]; Chew and Phoon [3]; Cao et al. [4]) were carried out to investigate the influence of embankment height, pile cap size and reinforcement on soil arching effect.

Centrifuge model test takes both advantages of the scaled model test and prototype experiment. Tests (Barchard [5]; Zhang et al. [6]; Wang et al. [7]) showed that in GRPS embankment load transfer largely depended on reinforcement function; in piled embankment without basal reinforcement, load transfer mainly depended on soil arching effect.

Existing researches concerned more about pile efficacy and pile-soil stress ratio (Han and Gabr [8]; Briancon et al. [9]; Van Eekelen et al. [10]), however considered little about the function of geosynthetic-reinforced mattress as a whole and its influencing factors. For these reasons, a series of 4 centrifuge model tests were applied to investigate the basal reinforcement effects on GRPS embankment. The results of load distribution and deformation were presented and analyzed. The influencing factors including reinforcement settings, position and the properties of reinforcing material were explored. The conclusions are used to provide guidance on reasonable establishment of GRPS embankment design.

## 2 Centrifuge Model Test

The prototype embankment was 6 m high, 16 m wide on the surface, and the slope ratio was 1:1.5. The filling process of the embankment was divided into three steps, and each step had a 2 m instantaneous load followed by 60-day repose as a transitional period. Reinforced concrete piles used in the GRPS embankment were 16 m in length, 0.5 m in diameter and 2.8 m in pile spacing with square disposing mode. Pile caps (1.6 m × 1.6 m) were fixed onto the piles. The basal reinforced cushion was 0.6 m thick and the tensile strength of bi-direction geogrid was 80 kN/m at a tensile strain of 5%. The thickness of soft soil foundation was 16 m, and the bearing stratum was sandy soil layer. The selected model ratio  $N$  equaled 80.

The number of geogrid layers was systematically analyzed in this experimental research plan. Four comparative tests were arranged including one non-reinforced piled embankment. Table 1 lists the tests that were conducted.

The model foundation of the centrifuge tests was composed of two layers, with soft soil layer over sand layer. The soft soil was silty clay which is a mixture of silty clay

**Table 1.** Test program of GRPS embankment.

Tests	Number of layers in the mattress	Layout of geogrid
G1	0	None
G2	1	Middle of the mattress
G3	2	Uniform distribution
G4	4	Uniform distribution

and mucky clay in Shanghai. The preparation of the soil included the process of drying, smashing, sieving and mixing with water into a paste. Then the soil sample was placed into the centrifugal field (80 g) to undergo the self-weight consolidation. The undrained shear strength ( $C_u$ ) of the soil was 12.6 kPa and the plasticity index of the soil was 15, and the modulus of compression ( $E_{s0.1-0.2}$ ) equaled 2.71. The permeability coefficient was  $7.56 \times 10^{-9}$  m/s. Sand with good grading distribution was used both for the mattress and the embankment fill. The particle size, less than 1 mm, was required to be as fine as possible because of the magnified effect in centrifuge model test. The model embankment was prepared by layers, and each layer was 1 cm thick. The volume of every layer was calculated through the embankment section area. The uniformity and compactness of the embankment were guaranteed through controlling the dry density of  $1.62 \text{ g/cm}^3$  under compaction. The lower layer of soil foundation simulated the bearing stratum of piles.

Figure 1 shows the size of the model and the layout of the instrumentations. The measuring components included three displacement sensors (s1–3) to monitor settlement at the road center, road shoulder and slope toe, respectively. An eddy displacement sensor, combined with a pre-placed board (s4), was applied to measure the horizontal displacement at 25–50 mm below the foot of the slope. Five earth pressure cells (epc1–5) were embedded to measure the load on pile and soil pressure over and below the reinforced mattress, aiming to study the load distribution through soil arching and tensioned membrane effect. The strains of geogrid were detected by four grid strain gauges (sg1–4) fixed with geogrid using epoxy as medium. It should be noted that the strain gauges stuck on the geogrids were calibrated before the tests.

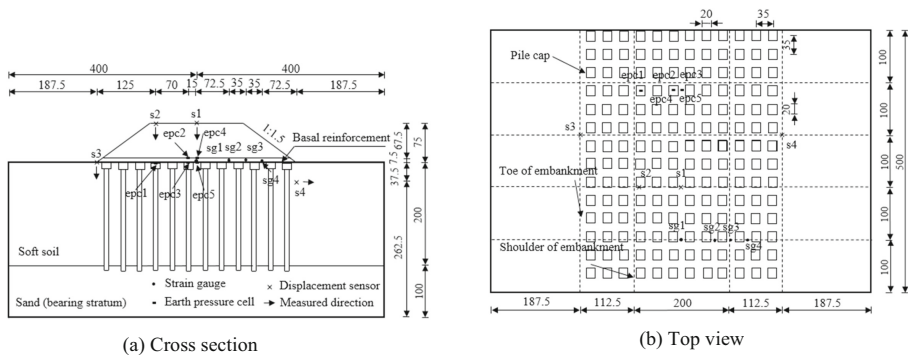


Fig. 1. Dimensions of models and arrangement of instruments (unit: mm).

After the foundation soil was in place, the following steps were carried out in each test: (1) consolidating soft soil foundation in the 80 g-centrifugal field for 5 h; (2) inserting model piles into predetermined positions vertically and precisely; (3) burying the soil pressure cells flatly in the mattress which should be carefully paved; (4) preparing the embankment according to the scheduled size by layers; (5) positioning displacement

sensors to measure the displacement and settlement of the specified locations. The variable acceleration loading method was taken to simulate the process of step-heaped loading exactly according to the prototype. Detailed time history of acceleration is shown in Fig. 2.

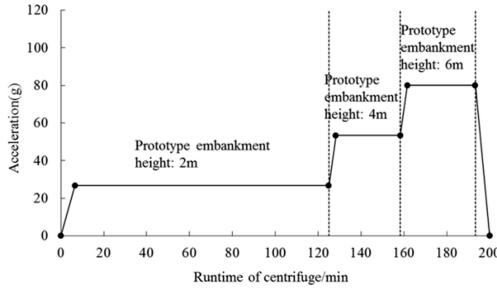


Fig. 2. Loading curve of models.

### 3 Analysis of Test Results

This section elaborates the analysis of the test results in prototype dimensions except the runtime of centrifuge for unified description.

#### 3.1 Deformation and Stability of Embankment

Figure 3 presents the settlement at the center of the embankment surface. It proves that the center settlement of non-reinforced piled embankment was far greater than those of reinforced and piled embankments. The former reached 1.46 m, while the latter ranged between 0.20–0.31 m when runtime of centrifuge was 180 min, which means the construction of the embankment was completed. It shows that the adoption of geogrid helped to decrease the vertical displacement. Moreover, the embankment settlement decreased with adding reinforcement layers, but the reinforcement effect of the mattress with 4 layers of geogrids was not so obvious compared to that with 2 layers. For 1 layer

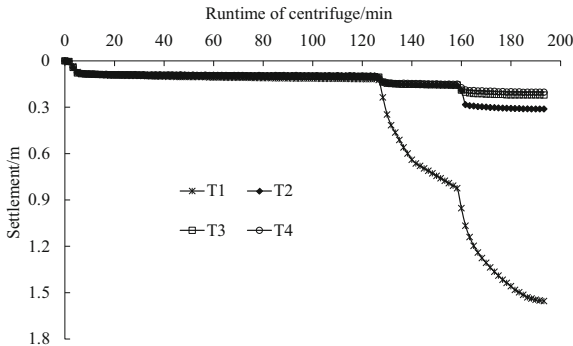


Fig. 3. Settlement curve of the center of the surface of the embankment.

of reinforcement, geogrid would have a stronger restriction effect on the settlement when paved in the middle of the mattress, where the soil-geogrid interaction could be better performed.

Figure 4 shows the differential settlement calculated by the embankment surface settlement of center ( $s_1$ ) and edge ( $s_2$ ), which depicted that the non-uniform settlement of embankment could be reduced effectively by the increasing of reinforcing layer number. Thus, the embankment integrity was also improved.

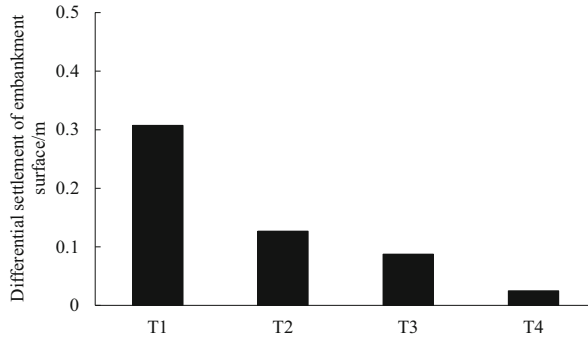


Fig. 4. Differential settlement of embankment surface between center and shoulder of the road (runtime of centrifuge: 180 min).

The stability of embankment on soft ground can be reflected by the ratio ( $\eta$ ) of maximum lateral displacement at the foot of embankment slope to the maximum settlement of subsoil surface (Chai [11]; Fei and Liu [12]). A rapid increase of this ratio means that the embankment is close to failure. Hence, quantitative evaluation of embankment stability can be done through the experimental result analysis. The maximum vertical displacement and lateral displacement of foundation soil in the test were measured by  $s_3$  and  $s_4$  separately. Figure 5 demonstrates the relationship between the ratio ( $\eta$ ) and the embankment filling height of prototype ( $H$ ).

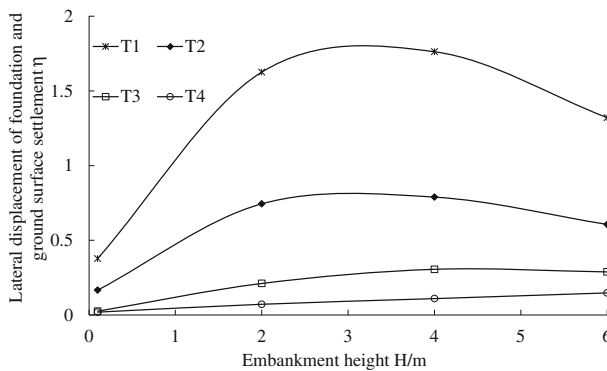


Fig. 5. Relationship between the ratio of lateral displacement of foundation and ground surface settlement to embankment height.

Figure 5 shows that with embankment height increasing, the trend of  $\eta$ - $H$  curves of models with 2 layers (T3) and 4 layers (T4) of geogrids were similar, that is, the ratio  $\eta$  slightly increased with embankment height and then stayed stable. A sharp increase of  $\eta$  in the height of 0–3 m appeared in the non-reinforced piled embankment (T1), which means that instability and large deformation occurred. Although the ratio decreased afterwards, it still maintained a large value. The embankment reinforced with 1 layer geogrid in the mattress (T2) underwent a quick rise in the initial stage of heap loading, while the magnitude was not as large as that in non-reinforcement embankment.

The above results show that the reinforcement in the mattress could reduce the embankment surface settlement and differential settlement, improve the overall stability, reduce the deformation of the foundation, and play the role of lateral restriction. Different reinforcement layers had great impacts on the effect of basal reinforcement in GRPS embankment and consequently had significant influence on the deformation of piled embankment.

### 3.2 Soil Arching Effect and Tensioned Membrane Effect

Pile efficacy (Hewlett and Randolph [1]), the ratio of embankment load on one pile to the total load in the processing range of a single pile, is utilized frequently in recent years to evaluate the soil arching effect. But there was no geosynthetic in their paper. In this paper, geosynthetic was used, so pile efficacy is illustrated by two calculations. The equations are as follows,

Above the reinforced mattress:

$$E_{pa} = \frac{ep_2 \times a^2}{[\gamma \times (H - d) + q] \times s^2} \quad (1)$$

Below the reinforced mattress:

$$E_{pb} = \frac{ep_3 \times a^2}{[\gamma \times (H - d) + \gamma' \times d + q] \times s^2} \quad (2)$$

The explanation of each symbol is shown in Fig. 1. In fact, the pile efficacy  $E_{pa}$  calculated using the pressure measurements above the mattress simply demonstrates the role of soil arching, while  $E_{pb}$  calculated using the measurements below the mattress demonstrates both the soil arching effect and the tensioned membrane effect.

A relationship can be found between  $E_{pa}$  and the filling height of the embankment, and so as to  $E_{pb}$ , which are both illustrated in Fig. 6. The result of T1 is not presented, because there was no reinforcement in the embankment mattress. In the upper half of Fig. 6, with the filling height increasing,  $E_{pa}$  became greater. The results of models T2–T4 were relatively close, indicating that the different settings of geogrid had little influence on soil arching effect.

In the lower half of Fig. 6,  $E_{pb}$  increased with the filling height, and the values of models T2–T4 reached 56.9%–64.2% under full load. On one hand, the results reveal

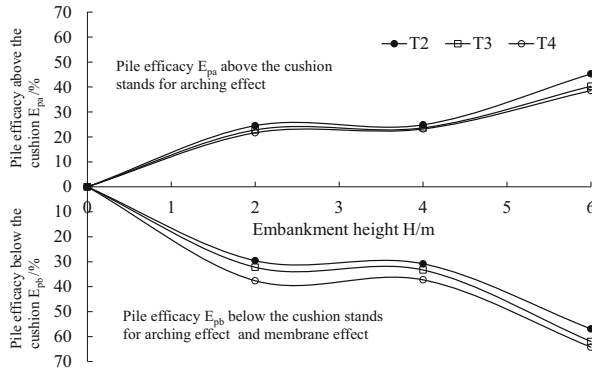


**Fig. 6.** Relationship between pile efficacy above the reinforcement and the increment in the center and embankment height.

that the role of reinforced mattress was to increase the load shared by the pile, and further exerted the bearing capacity of the pile. On the other hand, it indicates that the tensioned membrane effect of reinforcement was affected by the number of reinforcement layers.

### 3.3 Tensile Force of the Geogrid

The tensions of the geogrid were measured by four strain gauges (sg1–4) stuck on geogrids between the piles in the experiments. In mattress with more than one layer reinforcement, the strain gages were pasted on the bottom layer of the geogrids. The sg4 measurement of T4 was abnormal and was not adopted for analysis.

Figure 7 shows the distribution of reinforcement tension after full load of the embankment. It reveals that the tensile force measured by sg1 at the center of embankment and sg4 close to the foot of the slope were relatively small, while the tensile forces measured close to road shoulder by sg2 and sg3 were larger, which corresponded with the results reported by Zhang et al. [6]. The tensile force of the geogrid was influenced by two factors: the self-weight of the embankment fill between piles and the lateral slip of the embankment slope. The lateral slip of the embankment slope generated less tension of geogrid at the embankment center. The effect of self-weight of the embankment fill between piles was less obvious for geogrid close to the slope foot. Both of the two factors caused the large tensile force of geogrid under the road shoulder. The test results shown in Fig. 7 illustrate that, for the tensile force measured in the same location and with the same tensile modulus of the geogrid, its value got largest in the case with one reinforced layer at the middle of mattress (T2), and the case with multi-layers (T3, T4) came last. It is believed that in multi-layer reinforced embankment, the load was undertaken by all the layers and the tensile force of each single layer was reduced.

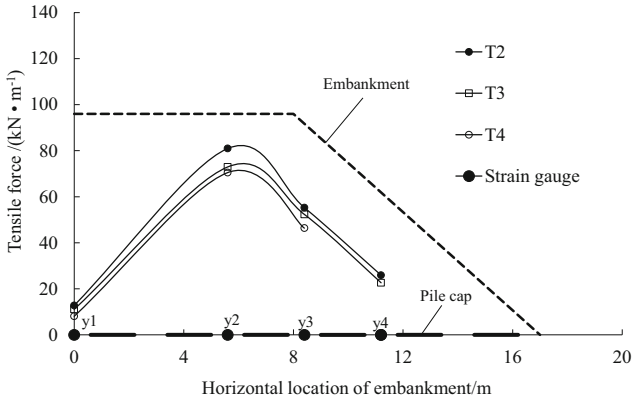


Fig. 7. Distribution of tensile force in belt (runtime of centrifuge: 180 min).

## 4 Conclusions

Four centrifuge model tests were performed on the role of basal reinforcement in GRPS embankment. The model test results were presented and analyzed, and the following conclusions can be drawn:

- (1) The surface settlement and differential settlement of embankment could be effectively reduced through appropriate setting of reinforced mattress.
- (2) The role of reinforced mattress was to increase the load shared by the pile and further exerted the bearing capacity of the pile. The tensioned membrane effect of reinforcement was affected by the number of reinforcement layers.
- (3) Geosynthetic basal reinforcement contributes to a GRPS embankment system in two ways, i.e., the lateral restraint and tensioned membrane effect. The former restricts the embankment lateral deformation and improved its stability, while the latter acts as an uplifting force to the overlying filling between piles, and transfers the load it takes onto the piles through tensioned membrane effect. Due to the lateral restraint of basal reinforcement, the tensile force of geogrid below the embankment shoulder was larger than that in the road center.

**Acknowledgment.** Financial support for this work is gratefully acknowledged from the Natural Science Foundation of China Grant 41772284 and Natural Science Foundation of Guangxi Grant 2015GXNSFBA139236. All the support is greatly appreciated.

## References

1. Hewlett, W.J., Randolph, M.F.: Analysis of piled embankments. *Ground Eng.* **22**(3), 12–18 (1988)
2. Low, B.K., Tang, S.K., Chao, V.: Arching in piled embankments. *J. Geotech. Geoenvironmental Engineering, ASCE* **120**(11), 1917–1938 (1994)



3. Chew, S.H., Phoon, H.L.: Geotextile reinforced piled embankment-full scale model tests. In: Proceeding of the 3rd Asian Regional Conference on Geosynthetics, pp. 661–668 (2004)
4. Cao, W.P., Chen, R.P., Chen, Y.M.: Experimental investigation on soil arching in piled reinforced embankments. *Chin. J. Geotech. Eng.* **29**(3), 436–441 (2007)
5. Barchard, J.M.: Centrifuge Modelling of Piled Embankments on Soft Soils. University of New Brunswick, Fredericton (1999)
6. Zhang, L., Luo, Q., Pei, F.Y., Yang, Y.: Bearing stratum effect at pile end of pile-cap-net structure subgrade based on centrifugal model tests. *Chin. J. Geotech. Eng.* **31**(8), 1192–1199 (2009)
7. Wang, C.D., Wang, B.L., Wang, X., Zhou, S.H.: Analysis on settlement controlling effect of pile-net composite foundation on collapsible loess by centrifugal model tests. *J. Chin. Railw. Soc.* **33**(4), 84–92 (2011)
8. Han, J., Gabr, M.A.: Numerical analysis of geosynthetic-reinforced and pile-supported earth platforms over soft soil. *J. Geotech. Geoenvironmental Eng.* **128**(1), 44–53 (2002)
9. Briançon, L., Delmas, P.H., Villard, P.: Study of the load transfer mechanisms in reinforced pile-supported embankments. In: Proceedings of 9 ICG, Brazil, pp. 1917–1920 (2010)
10. Van Eekelen, S.J.M., Benzuijen, A., Jansen, H.L.: Piled embankment using geosynthetic reinforcement in the Netherlands: design, monitoring & evaluation. In: Proceedings of the 17th International Conference on Soil Mechanics and Geotechnical Engineering, pp. 1690–1693 (2009)
11. Chai, J.C., Miura, N., Shen, S.L.: Performance of embankments with and without reinforcement on soft subsoil. *Can. Geotech. J.* **39**(4), 838–848 (2002)
12. Fei, K., Liu, H.L.: Field test study and numerical analysis of a geogrid-reinforced and pile-supported embankment. *Rock Soil Mech.* **30**(4), 1004–1012 (2009)